J Mater Sci (2012) 47:4167–4177
DOI 10.1007/s10853-012-6271-z

Impact of bleaching pine fibre on the fibre/cement interface

G. H. D. Tonoli · M. N. Belgacem · J. Bras · M. A. Pereira-da-Silva · F. A. Rocco Lahr · H. Savastano Jr.

Received: 21 September 2011 / Accepted: 11 January 2012 / Published online: 28 January 2012

Abstract The goal of this article was to evaluate the surface characteristics of the pine fibres and its impact on the performance of fibre–cement composites. Lower polar contribution of the surface energy indicates that unbleached fibres have less hydrophilic nature than the bleached fibres. Bleaching the pulp makes the fibres less stronger, more fibrillated and permeable to liquids due to removal the amorphous lignin and its extraction from the fibre surface. Atomic force microscopy reveals these changes occurring on the fibre surface and contributes to understanding the mechanism of adhesion of the resulting fibre to cement interface. Scanning electron microscopy shows that pulp bleaching increased fibre/cement interfacial bonding, whilst unbleached fibres were less susceptible to cement precipitation into the fibre cavities (lumens) in the prepared composites. Consequently, bleached fibre-reinforced composites had lower ductility due to the high interfacial adhesion between the fibre and the cement and elevated rates of fibre mineralization.

G. H. D. Tonoli (✉)
Department of Forest Science, Universidade Federal de Lavras, C.P. 3037, Lavras, MG 37200-000, Brazil
e-mail: gustavotonoli@yahoo.com.br

M. N. Belgacem · J. Bras
Laboratoire de Génie des Procédés Papetiers (LGP2), UMR CNRS 5518, Grenoble INP-Pagora—461, Rue de la Papeterie, 38402 Saint-Martin-d'Hères, France

M. A. Pereira-da-Silva
Instituto de Física de São Carlos, Universidade de São Paulo, C.P. 369, São Carlos, SP 13560-970, Brazil

M. A. Pereira-da-Silva
Centro Universitario Central Paulista—UNICEP, São Carlos, SP 13563-470, Brazil

F. A. Rocco Lahr
Department of Structural Engineering, Escola de Engenharia de São Carlos, Universidade de São Paulo, Avenida Trabalhador São-Carlense, 400, São Carlos, SP 13566-590, Brazil

H. Savastano Jr.
Department of Food Engineering, Faculdade de Zootecnia e Engenharia de Alimentos, Universidade de São Paulo (USP), Avenida Duque de Caxias Norte, 225, Pirassununga, SP 13635-900, Brazil

Introduction

Wood fibre-reinforced cement-based materials have being increasingly used in most developing countries as more sustainable construction materials [1–4]. The bond between cellulose fibre and Portland cement is of physical (mechanical interlocking) or chemical (mainly hydrogen bonds) nature, or a combination of both [5]. Some previous studies suggested that the mechanical interlocking (or anchorage) between the surface of cellulose fibre and cement hydration products, plays a significant role in bonding formation amongst these phases [6–10]. The chemical composition of the virgin pulp fibres (cellulose, polyoses, lignins and extractives) and of the cement hydration products developed on the fibre surface also exerts critical influence on the fibre to cement adherence, and consequently on the mechanical performance of the ensuing composite [11–13].

In addition, the highly alkaline pore water within the fibre/cement interface can induce the stiffening of the cellulose fibres by means of the mineralization phenomenon proposed elsewhere [11, 14–16], which lead to significant losses in the mechanical performance of the composites. The optimal situation would be the protection of the cellulose fibres from water uptake, which can be achieved by less hydrophilic surfaces (either natural or

after an adequate treatment), and without losing the quality of the fibre bridging that is responsible for the composite ductility. Although some studies reported of possible compromise between water absorption (WA) and adhesion [17, 18], there is still a lack of information about the influence of the chemical nature and morphology of the surface of cellulose fibre. Different from the literature, results presented here are from composites produced via slurry-dewatering and pressing technique instead of cast-in-place [16, 19]. Slurry-dewatering and pressing technique permits obtain composites with lower final water/cement ratio than those obtained by cast-in-place, influencing cement hydration and possibly fibre degradation. Slurry-dewatering and pressing is a simulation of the Hatschek process, which is currently the most used in the industry for production of fibre–cement sheets [20]. This study also shows useful information about the surface and strength of the pine cellulose fibres, which is currently the most used cellulose pulp for air cured fibre–cement products [2]. The effect of pulp bleaching on the chemical nature and morphology of the pine fibre surface, on the fibre strength, and its consequence on the microstructure and macrostructure performance of fibre–cement produced by vacuum-dewatering and pressing have not been systematically examined in the literature. This would lead to better understanding of mechanisms that affect the performance and the degradation of cellulose fibre–cement materials produced via slurry-dewatering. The main objective of this study was to evaluate the surface properties of the pine cellulose fibres and its effect on the microstructure, physical and mechanical properties of the fibre–cement composites.

Materials and methods

Materials

Commercial bleached and unbleached pine (*Pinus elliottii*) kraft pulps were used in the experiments. Kappa number of the pulps was determined following the standard SCAN C 1:77 [21]. The total residual lignin content (TRLC) was calculated according to: TRLC = (kappa number)/6.546, as described by Laine et al. [22]. The amount of wood extractives of the pulps was estimated following the TAPPI T 204 cm-97 [23] standard. The mean intrinsic viscosity of the pulps was determined in cupriethylenediamine diluted solution [24].

High early strength Portland cement (OPC) Type III according to ASTM C150 [25] and ground carbonate material were used as the matrix of the fibre–cement composites. This type of cement is free from mineral additions (like blast furnace slag or pozzolans) and was selected because it minimizes the interference of those additions on the study upon fibre mineralization. Ground carbonate filler (GCF), commonly used in agriculture, was used as partial substitution of OPC in order to reduce costs concerning the production of the fibre–cement. Oxide compositions of the OPC and of the GCF were accomplished by X-ray fluorescence (XRF) spectrometry (PANalytical Axios-Advanced). Oxide compositions of the OPC and of the GCF are presented in Table 1. X-ray diffraction (XRD) was performed using a Philips MPD1880, radiation Cuα, 0.02 (2 h) step and 1 s counting time, for characterizing the mineral phases in the OPC (Table 1). Particle size distribution by laser granulometry (Malvern Mastersizer S long bed, version 2.19) was performed using ethanol as a dispersion medium. According to particle size distribution, 50% of the particles are smaller than 11.0 and 16.2 μm for OPC and GCF, respectively. Most of the particles (90%) are smaller than 27.3 and 64.4 μm for OPC and GCF, respectively.

Surface morphology of the pulp fibre

Multimode Nanoscope IIIa atomic force microscope Digital Instrument at tapping-mode (TM-AFM) was used to study the fibre surface topography, by means of height and phase imaging data acquired simultaneously. Silicon cantilever with a spring constant of around 70 N m^{-1} [26] and a scan area of 3 × 3 μm^2 were used and all the images were measured in atmospheric (air) environment (temperature ca. 25 °C and relative humidity between 50 and 65%). The higher areas of the fibres were selected for these measurements, as previously detailed by Tonoli et al. [4].

Table 1 Oxide composition (% by mass) of the cement (OPC) and of the GCF and the cement phases by XRD

	CaO	MgO	SiO_2	Al_2O_3	Fe_2O_3	Na_2O	K_2O	SO_3	MnO	P_2O_5	TiO_2
OPC[a]	63.5	3.1	19.4	4.1	2.3	0.2	1.1	3.0	–	–	–
GCF[b]	39.1	8.9	9.0	2.2	1.2	0.1	0.4	–	0.1	0.2	0.1

OPC phases by XRD: Ca_3SiO_5, MgO, $Ca(OH)_2$, $CaCO_3$, SiO_2, Ca_2SiO_4, $CaSO_4$, $Ca_2Al_2O_5$, $Al(OH)_3$

[a] Loss of ignition (1000 °C) = 3.3% in mass; [b] loss of ignition (1000 °C) = 38.7% in mass

The raw data images were processed and reconstituted using the software NanoScope® III (v. 5.12b43 2002).

Contact angle (CA), surface energy and water retention value (WRV) of the pulp fibre

CA measurements were carried out to analyse the surface energy of the pulps by depositing calibrated droplets of liquid with different polarities on the surface of cellulose hand sheets of the investigated pulps using a Pulmac ASF-C1 to prepare these sheets. The main characteristics of the liquids used in this study were previously given by Tonoli et al. [12]. The apparatus was a dynamic CA DataPhysics OCA absorption tester, equipped with a charge-coupled device (CCD) camera. The dispersive and polar components of the surface energy of the cellulose samples were determined according to Owens and Wendt [27] approach, as given by Eq. 1.

$$\gamma_L(1+\cos\theta) = 2\sqrt{\gamma_L^D\gamma_S^D} + \sqrt{\gamma_L^P\gamma_S^P} \quad (1)$$

where γ, γ^D and γ^P are the total, dispersive and polar surface energy, respectively. Subscripts L and S refer to the liquid drop (L) and the solid surface (S), and θ denotes the CA between the solid (cellulose hand sheets) substrate and the liquid drop.

The WRV of the pulp is an empirical measurement of the capacity of the fibres to retain water. It was established according to TAPPI UM–256 [28] standard.

Fibre mechanical and bonding properties

Cellulose hand sheets from unbleached and bleached pulps were prepared, using deionized water and following the procedures described by TAPPI T 205 sp-95 [29] standard. Tensile strength and tensile stiffness of the cellulose hand sheets were determined according to SCAN P 38:80 [30] and TAPPI T 494 om-96 [31], respectively. At least eight hand sheets were used for each test. The fibre strength and fibre bonding index were measured with a zero-span tester Pulmac Z2400-C1, according to the standard methods of TAPPI T 273 cm-95 [32] and T 231 pm-96 [33], respectively.

Production of the fibre–cement composites

Cement-based composites were reinforced with pine kraft unbleached and bleached pulps. Optimal fibre–cement formulation was chosen based on previous studies [34, 35]. The suspensions with approximately 20% of solids were prepared using the following constituents (percentage by dry mass): 10.0% of cellulose pulp, 77.2% of OPC, 12.8% of ground carbonate material and distilled water. The correspondent percentage by dry volume of the cellulose pulp is around 18%. The cement-based composites (flat pads), measuring 200 mm × 200 mm and around 6-mm thick, were produced at laboratory scale using slurry vacuum-dewatering process followed by pressing technique, as described in details by Tonoli et al. [4]. The final water/cement ratio reached after this process was around 0.3. The fibre–cement pads were immediately wet sealed in a plastic bag for the initial cure and kept at room temperature for 2 days, then immersed in lime-saturated water for 26 days. Pads were wet cut into four 165 mm × 40 mm flexural test specimens using a water-cooled diamond saw. Specimens were tested 28 days after production upon completion of the immersion curing.

Characterization of the fibre–cement composites

Scanning electron microscopy (SEM) equipped with backscattered electron (BSE) detector was used to examine cut and polished surfaces for characterization of the fibre to matrix interface. Cementitious phases were identified by the contrast of atomic number of different chemical elements using the BSE mode. Dark and light areas are related to lower and higher atomic numbers, respectively. Identification of the chemical composition in different spots and semi-quantitative analysis were carried out by energy-dispersive X-ray spectrometry (EDS) in order to complement the characterization of hydration products. EDS atomic mapping [12] was also performed in order to localize the carbon (C), calcium (Ca) and silicon (Si) atoms on the same polished surface specimens. The preparation of specimens for BSE and EDS analyses was accomplished with low pressure (25 kPa gauge) impregnation using epoxy resin (MC-DUR1264FF). BSE EDS samples were ground with silicon carbide (SiC) grinding paper as described by Tonoli et al. [4]. Polished samples were carbon coated before being analysed in a LEO Leica S440 microscope with acceleration voltage of 20 kV, current of 150 mA and working distance of 25 mm. In order to avoid contamination of the EDS analysis from surround phases, each spot analysed was located at least 2 μm away from materials clearly consisting of other phases [36]. The semi-quantitative EDS analyses were the average of several spot measurements.

The mercury intrusion porosimetry (MIP) technique was adopted to compare microstructure of the composites, as usually applied in the characterization of cement-based materials [37]. MIP was performed using Micromeritics Poresizer 9320 with pressure of up to 200 MPa. The parameters values for the mercury were assumed as 0.495 g cm^{-3} for the surface tension and 13534 kg m^{-3} for the real density. The stabilization time in both low and high pressure settings was 10 s. The advancing/receding

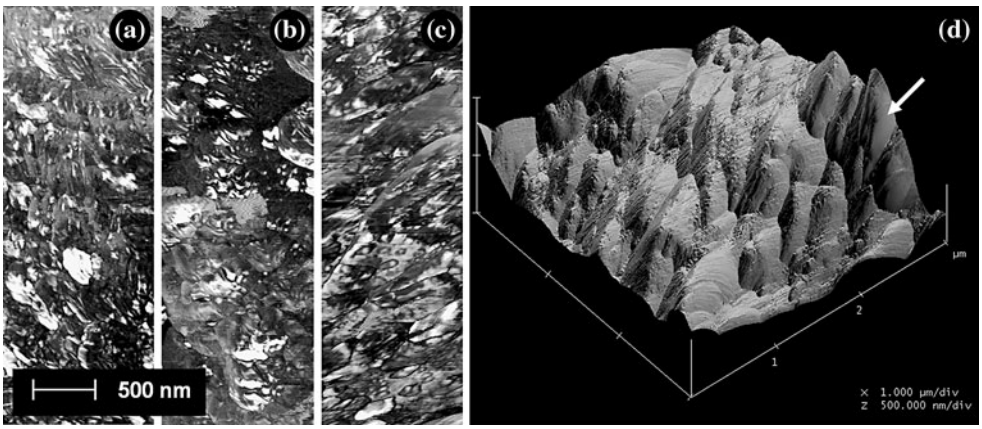

Fig. 1 **a–c** Typical AFM phase images in three unbleached pine fibres; **d** AFM topography image of unbleached pine fibre [image size is 3 µm × 3 µm × 500 nm (*z*)]. *Arrow* in (**d**) shows the granular structures that form the surface of the unbleached pine fibre

CA was assumed to be 130°. The amount of mercury intruded at each pressure interval was individually recorded. Specimens were cut with a cubic side length of approximately 5 mm, dried at 70 °C for 24 h and maintained in an air-tight receptacle before evaluation [38].

Physical properties, namely WA, apparent porosity (AP) and bulk density (BD) values were obtained from the average of six specimens for each design, following the ASTM C 948–81 [39] standard.

Mechanical tests were performed using the universal testing machine Emic DL-30,000 equipped with 1 kN load cell. Four-point bending configuration was employed to evaluate the limit of proportionality (LOP), modulus of rupture (MOR), modulus of elasticity (MOE) and specific energy (SE) of the specimens, as described elsewhere [12]. The deflection values were divided by the major span (135 mm) of the bending test, and called specific deflection (ε). The specific deflection at MOR (SDM) is the value of specific deflection at the point of higher stress (σ); it gives an indication of the capacity of deformation and toughness of the material under evaluation in the bending test. The composites were tested wet after immersion for 24 h in water in order to normalize for the humidity condition.

Results and discussion

Fibre surface properties of interest to fibre–cement interface

As it was expected, unbleached pulp contained higher amount of TRLC (~4.0% w/w) comparing to the negligible value determined in bleached counterpart (TRLC ~0.1% w/w). The amount of wood extractives was very similar and very low for both pulps (around 0.2% by mass). Bleaching of the pine kraft pulp resulted in surface modification of the fibres, although no significant changes were observed in the diameter and length of the fibres. As presented by the AFM micrographs (Fig. 1), granular structures were observed on the surface of unbleached pine fibres that are believed to be, associated with the presence of lignin and wood extractives [40, 41]. Gustafsson et al. [40] and Koljonen et al. [41] identified amorphous non-carbohydrates compounds on the fibre surface of slash pine and assigned them to the lignin and extractives content. Laine et al. [22] and Johansson [42] have used X-ray photoelectron spectroscopy (XPS) and established a lignin layer with thickness of about 10 nm on the fibres surface. In this study, the granular phase was correlated with the high TRLC as reported elsewhere [43].

Figure 2 (arrows) shows the typical fibrillar structures on the surface of the bleached fibres, with microfibrils measuring around 50 nm of average diameter, whilst the average diameter of the granular structures on the unbleached fibre surface is around 200 nm (arrow in Fig. 1d). In the fibre–cement composites, the higher the fibrillar surface of the fibres, the higher is their capacity to bond with the cement matrix [44].

Unbleached pine pulp had higher contact angles with water and other polar liquids like glycerol or ethylene glycol. This lead to lower surface energy compared to the bleached pine pulps (Fig. 3a).

Figure 3a presents the polar and dispersive contributions to the surface energy of unbleached and bleached pulps. Bleaching of the pulps increased the surface energy of the fibres, due to the increasing in the dispersive and polar components. The increase in the polar component and WRV (Fig. 3b) in bleached fibres indicates an improvement of their hydrophilic character due to the cleaning of the fibre surface from non-carbohydrates constituents of the fibres [45], such as wood extractives (surfactant-type molecules) and residual lignin.

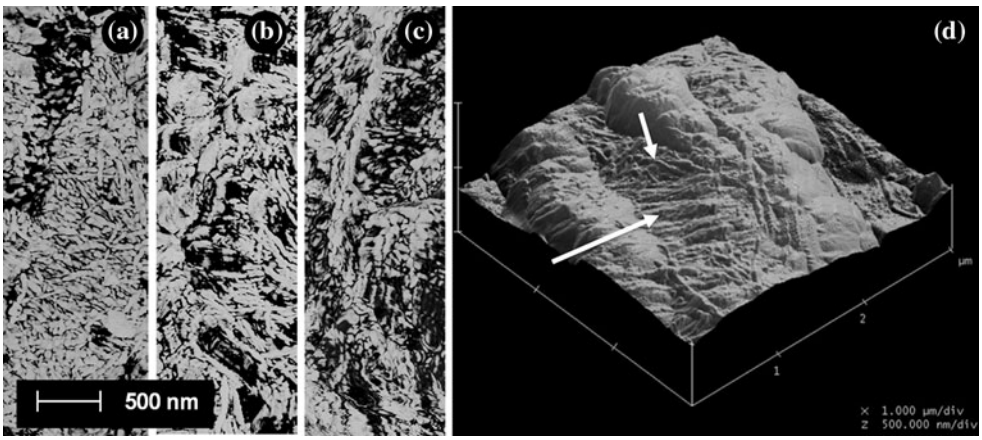

Fig. 2 **a–c** Typical AFM phase images in three bleached pine fibres; **d** AFM topography image of bleached pine fibre [image size is 3 μm × 3 μm × 500 nm (*z*)]. *Arrows* in (**d**) show the fibril-exposed surface that form the bleached pine fibre

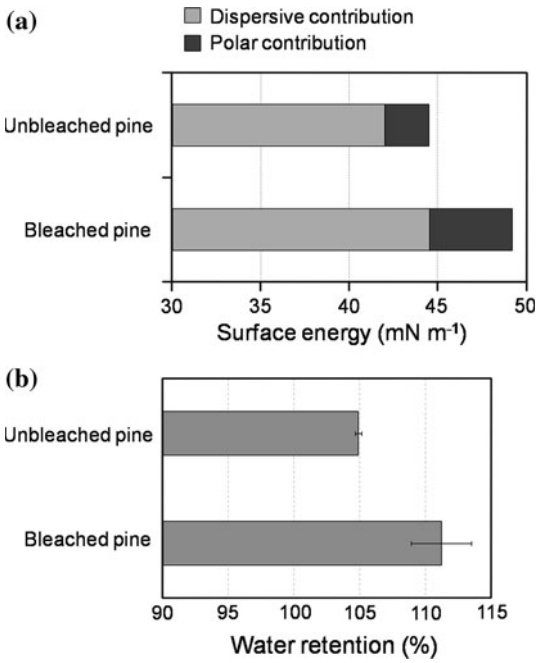

Fig. 3 **a** Surface energy components (polar and dispersive); and **b** average WRV and standard deviation of the unbleached and bleached fibres

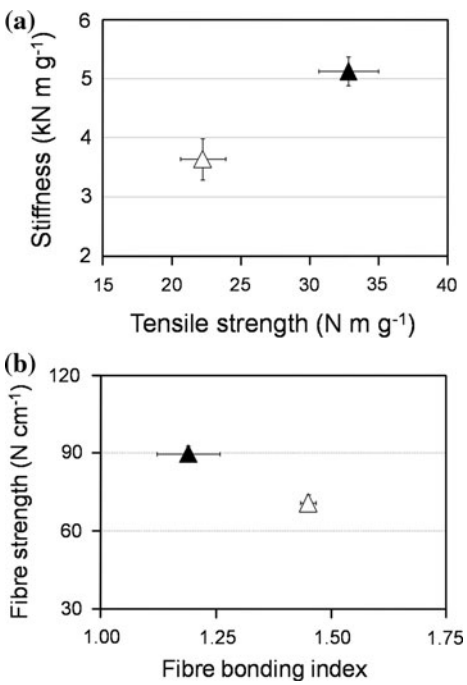

Fig. 4 Average and standard deviation values of **a** stiffness of cellulose hand sheets in function of their tensile strength and **b** fibre strength in relation to fibre bonding index. *Black* and *white triangles* are related to unbleached and bleached pine pulps, respectively

It is known that the bleaching reagents react mainly with lignin, breaking unsaturated bonds and producing carbonyl and carboxyl end structures and thereby increasing the hydrophilic character of fibres [46]. In the bleached pulps, the number of free OH groups in the fibre surface is higher than that exhibited by the surface of unbleached counterparts [47]. This can explain the reason why unbleached pine pulp had lower surface energy and WRV, when compared to the corresponding bleached pulp. The lower affinity of unbleached fibres to water is a remarkable surface property ensuring the preservation of the fibre from chemical degradation, since alkaline pore water is the main agent of fibre weakening within the cementitious matrix [48].

Figure 4 presents the strength characteristics of unbleached and bleached cellulose hand sheets. Tensile strength (Fig. 4a) of the cellulose hand sheets decreased with pulp bleaching because of decreasing the individual fibre strength (Fig. 4b) with carbohydrate depolymerisation reactions resulting from hydrolysis of glycosidic bonds and fibre structure defects induced by oxidation reaction that takes place during the bleaching procedures [49, 50]. This statement is supported by

the drop of the intrinsic viscosity caused by the decrease of cellulose chains with degradation observed for the studied fibres, before ($\sim$930 cm^3 g^{-1}) and after bleaching ($\sim$610 cm^3 g^{-1}). Other incremental remark is that bleaching also caused softening of fibre cell walls, resulting in a decrease of fibre stiffness (Fig. 4a) and presumably increasing of the diffusivity of the cement pore solution into the fibres. Despite the pulp strength loss with bleaching, the increased fibre bonding index (Fig. 4b) suggests the improvement in hydrogen bonding amongst the bleached fibres. This assertion is supported by the CA measurements, where the surface free energy of the bleached fibres is higher than that of unbleached homologues.

Effect of fibre surface on fibre–cement microstructure and physical properties

The SEM micrographs (BSE) of cut and polished fibre–cement sections after 28 days of cure are presented in Figs. 5 and 6. Despite the fibres seem to be shrunken in both composites series (unbleached and bleached), probably due to vacuum used during epoxy impregnation, the mineralization of the bleached fibres is evident. For the composites with unbleached pine pulp, the EDS spectra show a low amount of calcium (O/Ca ratio of 6.8 $\pm$ 1.1) in the fibre cell wall (spot 1 in Fig. 5b) and the lumens are free from visible deposition of cement hydration products (arrow in Fig. 5a). This phenomenon was attributed to the presence of macromolecular film rich in lignin and wood extractives on the fibre surface, correspondent to the residual media lamella. Thus, cement hydration in the unbleached fibre vicinities was severely inhibited, or was even stopped at the initial stage of cure, as observed by the voids around the fibres (arrow in Fig. 5b). This observation corroborates with the results of MIP (Table 2; Fig. 7), because the median pore diameter (Table 2) and the amount of mercury intruded in pores large than 0.1 μm (Fig. 7) were higher in composites reinforced with unbleached fibres.

Despite the limitations in provide a true pore size distribution, the MIP technique showed to be efficient as a comparative index of the pores at the transition zone between cellulose fibres and bulk matrix and in the fibre lumen, which pore sizes are in the range of 1–10 μm, as indicated by the microscopic examination (arrow in Fig. 5b). The smooth wavelike behaviour of the cumulative intrusion curves in Fig. 7 is an indicative of the ink-bottle pores effect in the cellulose fibre-reinforced composites, as also stated in the literature for other cement-based materials [51, 52]. Winslow and Diamond [53] brought the idea of a threshold pore radius based on the hypothesis that an initial percolating network of pores is formed when the size of the pores is equal to or larger than this threshold radius, and then mercury intrudes the innermost part of the sample. Most of the pores larger than the threshold radius should be intruded when the corresponding pressure is reached and the remaining intrusion presumably shows fewer characteristics of the ink-bottle effect [52]. In this study (arrow in Fig. 7), the mercury intrusion in the range of pores higher than 10 μm takes place in the unbleached fibre composite before than the bleached fibre composite. Therefore, the threshold pore radius for unbleached fibre composites is systematically higher than for bleached counterpart, clearly indicating the higher size of the pores disregarding the

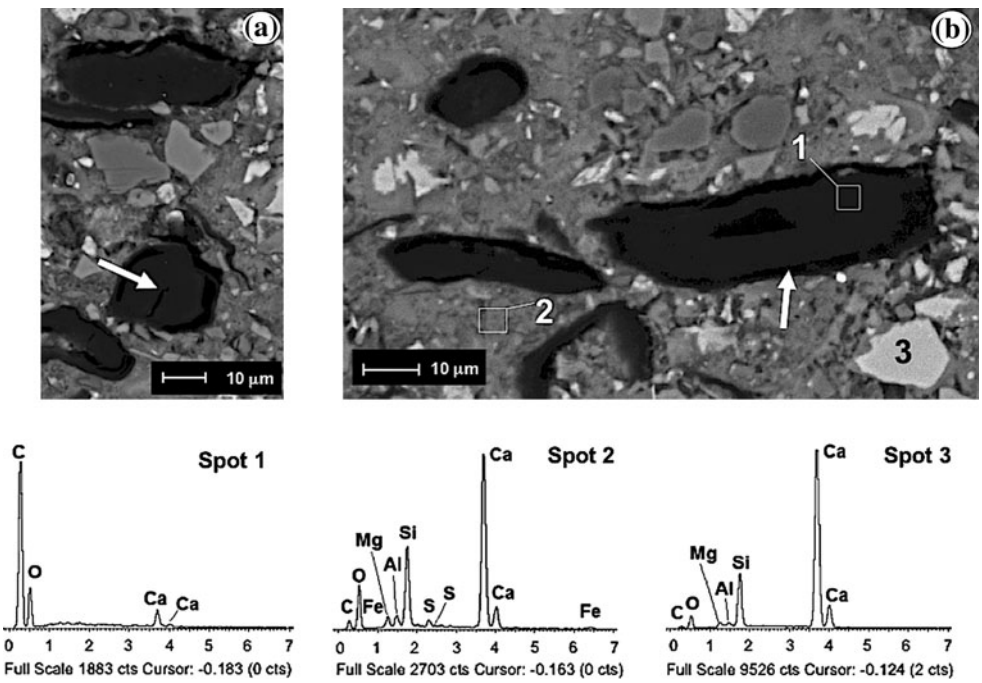

Fig. 5 Typical SEM BSE images of the polished surfaces of composites reinforced with unbleached pine pulp, after 28 days of cure (**a**, **b**). EDS spectra are signalized in the corresponding micrographs (spots *1–3*). *Arrows* in (**a**, **b**) show fibre lumen free from deposition of cement hydration products, and void around the fibre, respectively

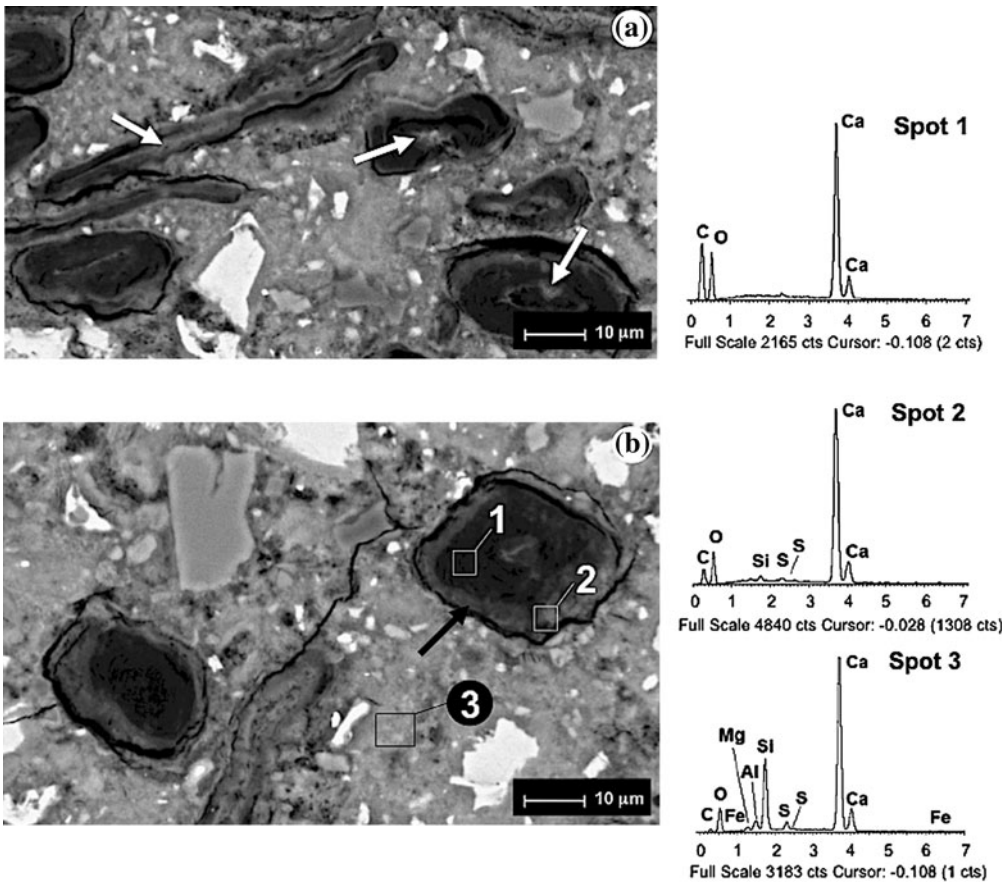

Fig. 6 Typical SEM BSE images of the polished surfaces of composites reinforced with bleached pine pulp, after 28 days of cure (**a, b**). EDS spectra (in the *right* column) are signalized in the corresponding micrographs (spots *1–3*). *Arrows* in (**a**) show cement hydration products precipitated in the fibre lumens

Table 2 MIP data of composites reinforced with unbleached and bleached pine pulps

Mercury intrusion porosimetry data	Unbleached	Bleached
Median pore diameter: volume (μm)	0.298 ± 0.015	0.111 ± 0.009
Median pore diameter: area (μm)	0.015 ± 0.009	0.016 ± 0.005
Average pore diameter: 4 V A^{-1} (μm)	0.06 ± 0.01	0.05 ± 0.01
BD (g cm^{-3})	1.52 ± 0.02	1.55 ± 0.01
Apparent (skeletal) density (g cm^{-3})	1.99 ± 0.03	2.05 ± 0.01

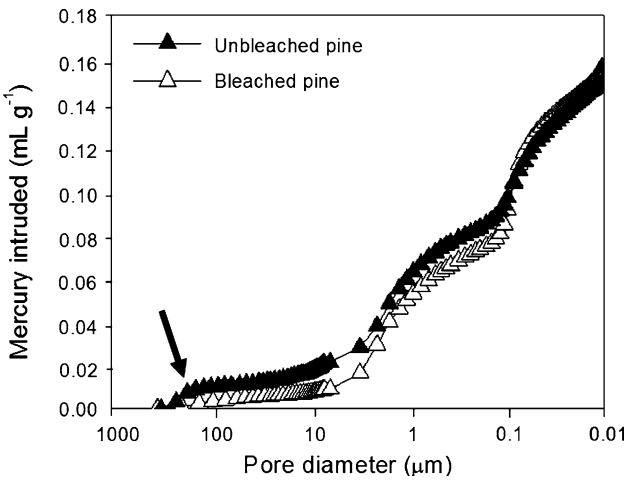

Fig. 7 Cumulative MIP of the composites reinforced with unbleached and bleached pine pulps. *Arrow* indicates the large mercury intrusion in higher pore sizes for unbleached fibre composite

actual volume of mercury intruded. According to Diamond [51], such MIP uses do appear to be valid as a comparative index within the restrictions imposed by the nature of the mercury intrusion technique.

According to the literature [54, 55], the minimum size of pores detected by MIP is about 7 nm. Mindess and Young [54] suggested that pores smaller than 10 nm do not contribute to water and ionic transport and therefore they were not considered in this article.

The film rich in lignin and extractives on the surface of unbleached fibres results in fewer Ca^{2+} and Si^{4+} and other ions released into the cement solution around these fibres and consequently lower rates of precipitation into the fibre lumens. Mohr et al. [19] reported that lignin and wood extractives play a protecting role against fibre mineralization in cast-in-place composites, acting as a chemical and physical barrier to the penetration of Ca^{2+} ions into the fibres. In this study, whose the composites were produced via slurry-dewatering, this chemical and physical barrier in unbleached fibres is equally important because difficult the

entrance of cement solution into the fibres during the vacuum steps throughout the fibre–cement manufacture. Moreover, the precipitation of cement hydration products around the unbleached fibres after 28 days of cure was practically inexistent, as evidenced by the arrow in Fig. 5b. The EDS spot analyses show that the elemental composition of the hydration products in the cement paste (spot 2, Fig. 5b) present Si/Ca ratio in the range of 0.28–0.43, S/Ca ratio in the range of 0.02–0.04 and Al/Ca ratio in the range of 0.05–0.08.

For the composites prepared with bleached fibres; the lumens are visibly filled by cement hydration products rich in calcium (arrows in Fig. 6a), and as evidenced by the EDS spectra (spots 1 and 2, Fig. 6b). The rougher fibrillated surface (Fig. 2d), and the higher surface energy (Fig. 3a) of the bleached fibres suggest their higher capacity of adhesion with other phases. In the bleached fibres, the lignin and wood extractives were practically fully removed, which allows the ion diffusion process at the fibre to cement interfacial zone. Cement ions move and precipitate at the fibre surface (spot 2, Fig. 6b) and permeate into the cell wall and the fibre lumens resulting in accelerated mineralization of the cell wall (spot 1, Fig. 6b). Such phenomenon occurred due to the high concentration gradients of cement ions at fibre surface [16]. Therefore, bleaching turned the fibres to be more susceptible to mineralization.

A large cement precipitation around the bleached fibres is observed. As a consequence, a decrease in the pores and spaces in their vicinities is induced as shown by the arrow in Fig. 6b and with the results of MIP (Fig. 7). The EDS spot analyses show that the elemental composition of the hydration products in the bleached fibre cell wall (spot 1, Fig. 6b) presents a O/Ca ratio of 3.4 ± 0.8, in the fibre lumen (arrows in Fig. 6a) and at the interface (spot 2, Fig. 6b) presents Si/Ca ratio in the range of 0.05–0.45, S/Ca ratio in the range of 0.01–0.08, and Al/Ca ratio in the range of 0.02–0.08. Cement paste (spot 3, Fig. 6b) in the composites with bleached fibres presents Si/Ca of 0.49 ± 0.01, S/Ca of 0.04 ± 0.01 and Al/Ca ratio of 0.08 ± 0.03. Based on this results, one could speculate that $Ca(OH)_2$ crystals and some sulphate-rich phases (e.g. monosulphate and ettringite) that exist in the fibre lumen and at the interface, may be beneficial to interlocking between fibre and cement. It could also result in better bond strength by means of intermolecular forces [15, 56, 57].

The higher precipitation rates in the fibre lumens and in the fibre to matrix interface with bleached fibres corroborates the results of MIP (Table 2) and physical properties (Table 3), where median pore diameter, WA and AP was lower and BD and apparent (skeletal) density was higher in the bleached fibre-reinforced composites, comparing to the same parameters observed for unbleached fibre-reinforced counterparts. The precipitation of hydration products, such as $Ca(OH)_2$ or sulphate-rich species, in the fibre–matrix transition zone, can restrain fibre swelling and shrinkage upon wetting and drying, respectively [19].

Table 3 Average and standard deviation values of physical properties of composites reinforced with unbleached and bleached pine pulps

Physical property	Composite	
	Unbleached pine fibres	Bleached pine fibres
WA (%)	23.2 ± 1.0	21.1 ± 1.2
AP (%)	33.8 ± 0.7	33.0 ± 1.2
BD (g cm^{-3})	1.46 ± 0.03	1.57 ± 0.04

Finally, in the EDS atomic mapping of the calcium atoms of the polished surfaces corresponding to bleached fibres-reinforced composites, calcium (green) is located within the fibre cell wall (Fig. 8d). The concentration of carbon (red) decreased in the fibre cell wall. In the composites reinforced with unbleached fibres, the carbon atoms are still present in great amount within the fibre cell wall (Fig. 8b). Thus, the components of fibre cell wall in the unbleached fibres seem to play an important role in minimizing the mineralization and degradation of the fibres during curing.

Effect of fibre surface properties on fibre–cement mechanical performance

Table 4 depicts the summary of the mechanical properties achieved with composites reinforced with unbleached and bleached pulps. LOP and MOR values do not seem to be influenced by the fibre bleaching, whilst MOE values increased with bleaching due to the increase of fibre to cement adherence. Mineralization of the fibre cell wall increases the affinity of the fibre surface to cement [16]. If fibres adhere more to the cement or their lumens are filled with cement precipitations, the incidence of pulled-out fibres is drastically reduced in a more packed structure in the composites (Table 2). Then, fibre rupture may occur and the fibre–cement composites absorb less energy from fibre to cement friction [9, 10]. For this reason, pulp bleaching decreased the values of SE and SDM of the fibre–cement composites (Table 4).

The fact that unbleached fibres present smoother surface, lower surface energy, higher fibre strength and absence of precipitation in their boundaries provides them the capacity to dissipate higher energy through the mechanism of pull out than their bleached counterparts. Consequently, composites reinforced with unbleached fibres had higher values of SE and SDM (Table 4). Also, unbleached fibres in the composites were usually free from

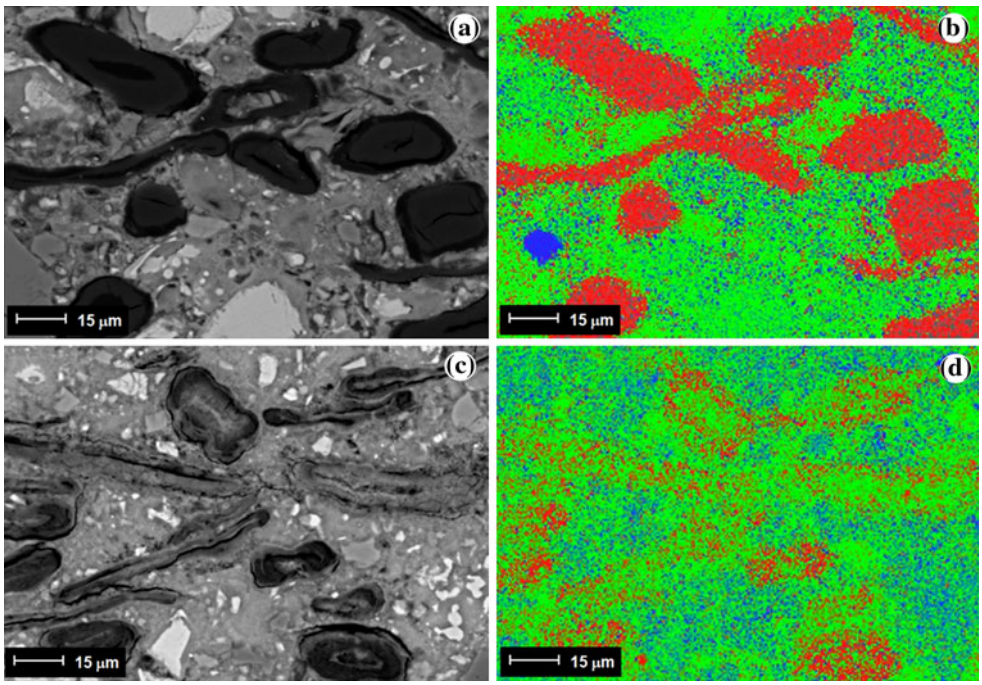

Fig. 8 Typical SEM BSE images (*left*) and EDS atomic mapping (*right*) of C (*red*), Ca (*green*) and Si (*blue*) of the polished surfaces of composites reinforced with **a**, **b** unbleached pine fibres and **c**, **d** bleached pine fibres. Images obtained after 28 days of cure (Color figure online)

Table 4 Average and standard deviation values of mechanical properties of composites reinforced with unbleached and bleached pine pulps

Mechanical property	Composite	
	Unbleached pine fibres	Bleached pine fibres
LOP (MPa)	5.0 ± 0.5	5.7 ± 1.4
MOR (MPa)	9.9 ± 1.2	9.4 ± 1.4
MOE (GPa)	8.6 ± 1.4	10.0 ± 0.5
SE (kJ m^{-2})	4.9 ± 0.4	3.5 ± 1.1
SDM (μm mm^{-1})	67.5 ± 12.0	33.3 ± 6.0

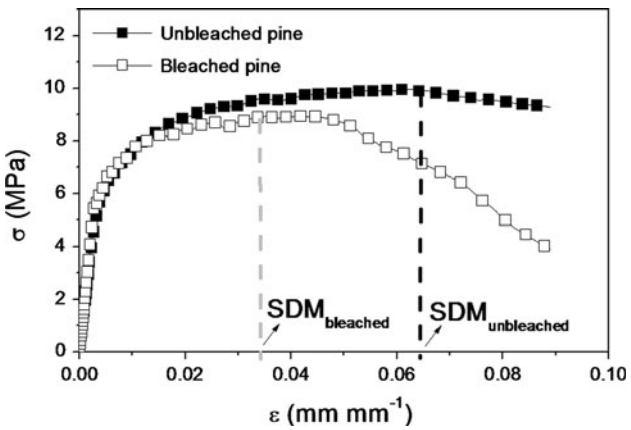

Fig. 9 Typical stress versus specific deflection curves for composites reinforced with unbleached and bleached pine pulps, after 28 days of cure

hydration products in their cavities (lumen), as evidenced by the EDS spectrum with high carbon content (spot 2, Fig. 5b) and by the EDS atomic mapping (Fig. 8a, b), which makes them more flexible and less brittle than the bleached homologues.

Figure 9 shows the comparison between the typical stress versus specific deflection curves of the fibre–cement composites. In both samples, the presence of fibre guaranteed the pseudo-plastic behaviour of the composites at the age of 28 days, with the peak strength (MOR) occurring after the first crack strength (LOP). However, composites reinforced with bleached pulp fibres exhibited a fracture process less stable because they presented a major drop in the post-cracking region, comparing to the composites reinforced with unbleached pulp, as illustrated in Fig. 9. In the case of bleached fibres, the adhesion could be higher than the fibre's strength and therefore they may rupture, instead of performing the complete frictional slip process.

Conclusion

AFM and surface energy measurements demonstrate clearly the changes on the fibre surface owing to bleaching. Fibres with lower polar contribution to the surface energy, that was the case of unbleached pine fibres, presented lower WRV, suggesting they are less hydrophilic than bleached counterpart. Unbleached fibres have high strength and stiffness, and present a thin lignin and extractives-rich layer on their surface, which reduces water intake and acts as a physical and chemical barrier to cement penetration into the fibre cavities (lumens). As a result, unbleached pulps were less susceptible to mineralization after curing in the fibre–cement composites. Different from the literature,

results presented here are from composites produced via slurry-dewatering and pressing technique, instead of cast-in-place. The lumens of the bleached fibres are filled with cement hydration products, probably $Ca(OH)_2$- and sulphate-rich present phases, and presented an improved fibre to cement adherence due to the fibril-exposed surface and precipitation of that cement hydration products in the fibre vicinities. MIP and microscopic examination show comparatively the impact of bleaching on the composite microstructure. Fibres that strongly adhere to cement will rather fracture instead of being pulled out from the matrix with greater dissipation of energy. Consequently, fibre–cement composites reinforced with bleached pulp presented lower toughness than those made with unbleached homologues. This contribute to better understanding of the impact of fibre surface properties on the fibre–cement interface, on the composite performance and on the mechanisms that affect the degradation of cellulose fibre–cement materials produced via slurry-dewatering. In general, the use of bleached instead of unbleached pine fibres allows obtaining stiffer but more brittle composites. Otherwise, the use of unbleached instead of bleached pine fibres contemplates a cheaper cellulose fibre alternative, providing economy in the manufacture and presumably improvements in the durability of the fibre–cement product.

Acknowledgements Financial support for this research project was provided by Conselho Nacional de Desenvolvimento Científico e Tecnológico (CNPq) and Fundação de Amparo à Pesquisa do Estado de São Paulo (Fapesp) in Brazil. The authors were supported by grants offered by CNPq and Fapesp (Process n° 2005/59072-4). The authors also thank Fibria Celulose S. A., Infibra Ltda. and Imbralit Ltda., in Brazil.

References

1. Sudin R, Swamy N (2006) J Mater Sci 41:6917. doi:10.1007/s10853-006-0224-3
2. Ikai S, Reichert JR, Rodrigues AV, Zampieri VA (2010) Constr Build Mater 24(2):171. doi:10.1016/j.conbuildmat.2009.06.019
3. Tonoli GHD, Santos SF, Joaquim AP, Savastano H Jr (2010) Constr Build Mater 24(2):193. doi:10.1016/j.conbuildmat.2007.11.018
4. Tonoli GHD, Savastano H Jr, Fuente E, Negro C, Blanco A, Rocco Lahr FA (2010) Ind Crops Prod 31(2):225. doi:10.1016/j.indcrop.2009.10.009
5. Coutts RSP (1988) In: Swamy RN (ed) Natural fibre reinforced cement and concrete (concrete technology and design, 5). Blackie, Glasgow, pp 208–242
6. Coutts RSP, Kightly P (1984) J Mater Sci 19:3355. doi:10.1007/BF00549827
7. Michell AJ, Freischmidt G (1990) J Mater Sci 25(12):5225. doi:10.1007/BF00580155
8. Bentur A (2000) J Mater Civ Eng 12(1):2
9. Savastano H Jr, Warden PG, Coutts RSP (2003) Cem Concr Compos 25(6):585. doi:10.1016/S0958-9465(02)00071-9
10. Savastano H Jr, Warden PG, Coutts RSP (2005) Cem Concr Compos 27(5):583. doi:10.1016/j.cemconcomp.2004.09.009
11. Mohr BJ, Nanko H, Kurtis KE (2005) Cem Concr Compos 27(4):435. doi:10.1016/j.cemconcomp.2004.07.006
12. Tonoli GHD, Rodrigues Filho UP, Savastano H Jr, Bras J, Belgacem MN, Rocco Lahr FA (2009) Compos A 40(12):2046. doi:10.1016/j.compositesa.2009.09.016
13. Joaquim AP, Tonoli GHD, Santos SF, Savastano H Jr (2009) Mater Res 12(3):305. doi:10.1590/S1516-14392009000300010
14. Bentur A, Akers SAS (1989) Int J Cem Compos Lightweight Concr 11(2):99. doi:10.1016/0262-5075(89)90120-6
15. Tolêdo Filho RD, Scrivener K, England GL, Ghavami K (2000) Cem Concr Compos 22(2):127. doi:10.1016/S0958-9465(99)00039-6
16. Wei YM, Fujii T, Hiramatsu Y, Miyatake A, Yoshinaga S, Fujii T, Tomita B (2004) J Wood Sci 50(4):327. doi:10.1007/s10086-003-0576-0
17. Savastano H Jr, Agopyan V (1999) Cem Concr Compos 21(1):49. doi:10.1016/S0958-9465(98)00038-9
18. Yue Y, Li G, Xu X, Zhao Z (2000) Cem Concr Res 30(12):1983. doi:10.1016/S0008-8846(00)00376-8
19. Mohr BJ, Biernacki JJ, Kurtis KE (2006) Cem Concr Res 36(7):1240. doi:10.1016/j.cemconres.2006.03.020
20. Dias CMR, Savastano H Jr, John VM (2010) Constr Build Mater 24(2):140. doi:10.1016/j.conbuildmat.2008.01.017
21. SCAN standard (1977) C 1:77. Kappa Number. Stockholm, Sweden
22. Laine J, Stenius P, Carlsson G, Ström G (1994) Cellulose 1(2):145. doi:10.1007/BF00819664
23. TAPPI standard (1997) T 204 cm-97. Solvent extractives of wood and pulp. Atlanta, GA, USA
24. SCAN standard (1999) CM 15:99. Viscosity in cupriethylenediamine solution. Stockholm, Sweden
25. ASTM standard (2009) C 150-09: Standard Specification for Portland Cement. West Conshohocken, PA, USA
26. Digital Instruments (1996) Instruction manual for multimode scanning probe microscope. Santa Barbara. Version 4.22, pp 11–29
27. Owens DK, Wendt RC (1969) J Appl Polym Sci 13(8):1741. doi:10.1002/app.1969.070130815
28. TAPPI standard (1981) UM 256. Water retention value. Atlanta, GA, USA
29. TAPPI standard (1995) T 205 sp-95. Forming handsheets for physical test of pulp. Atlanta, GA, USA
30. SCAN standard (1980) P 38:80. Determination of tensile properties—Part 2: Constant rate of elongation method for pulp and paper. Stockholm, Sweden
31. TAPPI standard (1996) T 494 om-96. Tensile properties of paper and paperboard (using constant rate of elongation apparatus). Atlanta, GA, USA
32. TAPPI standard (1995) T 273 pm-95: Wet zero-span tensile strength of pulp. Atlanta, GA, USA
33. TAPPI standard (1996) T 231 om-96: Zero-span breaking strength of pulp (dry zero-span tensile). Atlanta, GA, USA
34. Tonoli GHD, Joaquim AP, Arsène M-A, Bilba K, Savastano H Jr (2007) Mater Manuf Process 22:149. doi:10.1080/10426910601062065
35. Tonoli GHD, Fuente E, Monte C, Savastano H Jr, Rocco Lahr FA, Blanco A (2009) Cem Concr Res 39(11):1017. doi:10.1016/j.cemconres.2009.07.010
36. Bonen D, Diamond S (1994) J Am Ceram Soc 77(7):1875. doi:10.1111/j.1151-2916.1994.tb07065
37. Mehta PK, Monteiro PJM (2006) Concrete: microstructure, properties, and materials, 3rd edn. McGraw Hill, New York
38. Tonoli GHD, Savastano H Jr, Santos SF, Dias CMR, John VM, Lahr FAR (2011) J Mater Civ Eng 23(2):177. doi:10.1061/(ASCE)MT.1943-5533.0000152

39. ASTM standard (1981) C 948-81: Test method for dry and wet bulk density, water absorption, and apparent porosity of thin sections of glass-fiber reinforced concrete. West Conshohocken, PA, USA
40. Gustafsson J, Ciovica L, Peltonen J (2003) Polymer 44:661. doi:10.1016/S0032-3861(02)00807-8
41. Koljonen K, Österberg M, Johansson L-S, Stenius P (2003) Colloids Surf A 228:143. doi:10.1016/S0927-7757(03)00305-4
42. Johansson L-S (2002) Microchim Acta 138:217. doi:10.1007/s006040200025
43. Simola J, Malkavaara P, Alen R, Peltonen J (2000) Polymer 41(6):2121. doi:10.1016/S0032-3861(99)00379-1
44. Coutts RSP (2005) Cem Concr Compos 27(5):518. doi:10.1016/j.cemconcomp.2004.09.003
45. Belgacem MN, Czeremuszkin G, Sapieha S, Gandini A (1995) Cellulose 2(3):145. doi:10.1007/BF00813015
46. Katz S, Scallan AM (1983) Tappi J 66(1):85
47. Kajanto I, Niskanen K (1998) In: Niskanen K (ed) Paper physics. Papermaking science and technology. Book 16. Fapet Oy & Tappi Press, Helsinki, pp 223–259
48. Tolêdo Filho RD, Ghavami K, England GL, Scrivener K (2003) Cem Concr Compos 25:185. doi:10.1016/S0958-9465(02)00018-5
49. Brown G, Dawe R (1996) In: International pulp bleaching conference, Tappi Press, Washington, pp 38–390
50. Torres LF, Melo R, Colodette JL (2005) Revista Árvore 29(3):489. doi:10.1590/S0100-67622005000300017
51. Diamond S (2000) Cem Concr Res 30:1517–1525. http://dx.doi.org/10.1016/S0008-8846(00)00370-7
52. Moro F, Bohni H (2002) J Colloid Interface Sci 246:135. doi:10.1006/jcis.2001.7962
53. Winslow DN, Diamond S (1970) ASTM J Mater 5:564
54. Mindess S, Young JF (1981) Concrete. Prentice-Hall, Englewood Cliffs 671
55. Zhou J, Ye G, Van Breugel K (2010) Cem Concr Res 40:1120. doi:10.1016/j.cemconres.2010.02.011
56. Chatterji S (1998) Adv Cem Based Mater 7(3–4):102. doi:10.1016/S1065-7355(97)00058-8
57. Rossetto HL, Souza MF, Pandolfelli VC (2009) Cerâmica 55(334):199. doi:10.1590/S0366-69132009000200013